Shear-Thinning Nanocomposite Hydrogels for the Treatment of Hemorrhage

Akhilesh K. Gaharwar § ǂ ǀ ^ ± †, Reginald K. Avery ⅂ ǀ, Alexander Assmann ⅁ ǀ ǂ ±, Arghya Paul ǂ ǀ ±, Gareth H. McKinley ⅃, Ali Khademhosseini ǀ ǂ ± *, Bradley D. Olsen § *

§ Department of Chemical Engineering, Massachusetts Institute of Technology, Cambridge, MA 02139 (USA)

ǂ Wyss Institute for Biologically Inspired Engineering, Harvard University, Boston, MA 02115 (USA)

ǀ Center for Biomedical Engineering, Department of Medicine, Brigham and Women's Hospital, Harvard Medical School, Cambridge, MA 02139 (USA)

± Harvard-MIT Division of Health Sciences and Technology, Massachusetts Institute of Technology, Cambridge, MA 02139 (USA).

^ David H. Koch Institute for Integrative Cancer Research, Massachusetts Institute of Technology, Cambridge, MA 02139 (USA)

⅂ Department of Biological Engineering, Massachusetts Institute of Technology, Cambridge, MA 02139 (USA)

⅃ Department of Mechanical Engineering, Massachusetts Institute of Technology, Cambridge, MA 02139 (USA)

⅁ Department of Cardiovascular Surgery, Heinrich Heine University, Medical Faculty, 40225 Duesseldorf (Germany)

Supporting Information

Table S1. Weight percent (w/w) composition of each nanocomposite hydrogel.

Sample Name	9NC0	9NC25	9NC50	9NC75	9NC100
Gelatin (wt%)	9	6.75	4.5	2.25	0
Nanoplatelets (wt%)	0	2.25	4.5	6.75	9
Water (wt%)	91	91	91	91	91

Sample Name	6NC0	6NC25	6NC50	6NC75	6NC100
Gelatin (wt%)	6	4.5	3	1.5	0
Nanoplatelets (wt%)	0	1.5	3	4.5	6
Water (wt%)	94	94	94	94	94

Sample Name	3NC0	3NC25	3NC50	3NC75	3NC100
Gelatin (wt%)	3	2.25	1.5	0.75	0
Nanoplatelets (wt%)	0	0.75	1.5	2.25	3
Water (wt%)	97	97	97	97	97

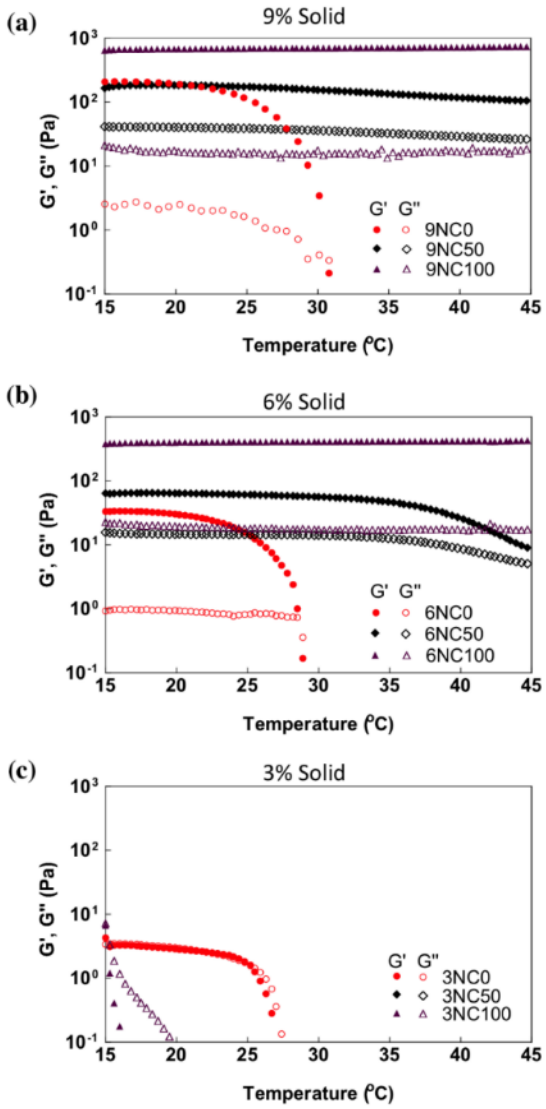

Figure S1. Effect of silicate nanoplatelets on thermal stability of nanocomposite hydrogels. Gelatin at lower temperatures is solid, but at higher temperature loses its mechanical integrity. Storage modulus (G') and loss modulus (G") of gelatin and nanocomposite hydrogels with solid concentrations of a) 9 wt%, b) 6 wt% and c) 3 wt% were monitored from 15 °C to 45 °C. Gelatin (NC0) was observed to flow at all solid concentrations above 32 °C. The addition of silicates improved the thermal stability of the nanocomposite network. All temperature sweeps were performed at a shear stress of 10 Pa and frequency of 1 Hz.

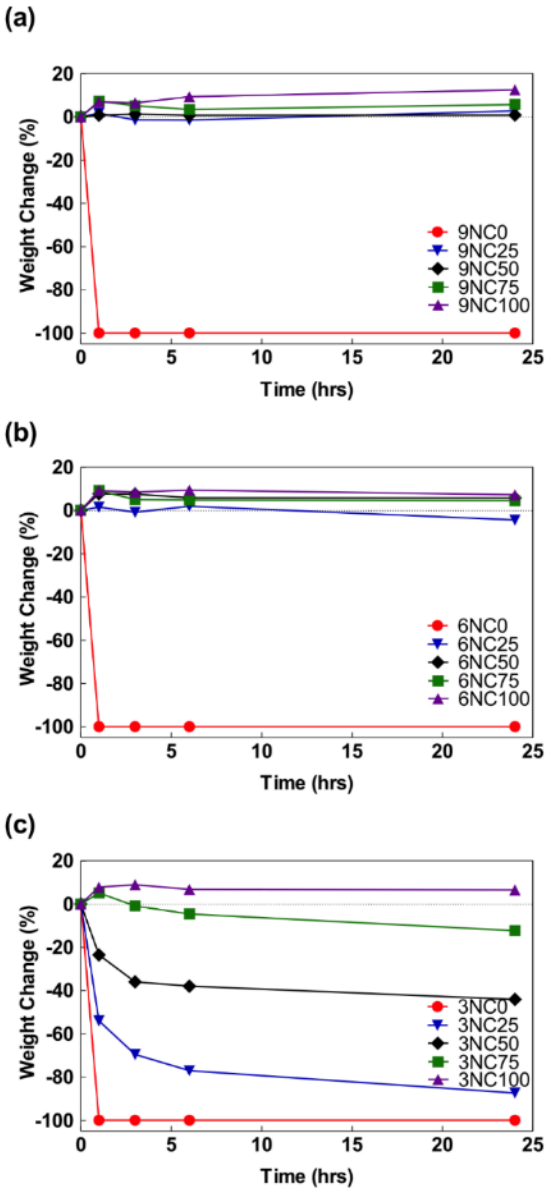

Figure S2. Effect of silicate nanoplatelet on the stability of nanocomposite hydrogels in physiological solution. Physiological stability was determined by measuring the weight of nanocomposites with solid concentration of a) 9 wt%, b) 6 wt% and c) 3 wt% stored in PBS at 37 °C. Gelatin (NC0) immediately dissolved in PBS, while nanocomposites of 6 wt% and 9 wt% solid concentrations maintained their structural integrity throughout the 24 hour test.

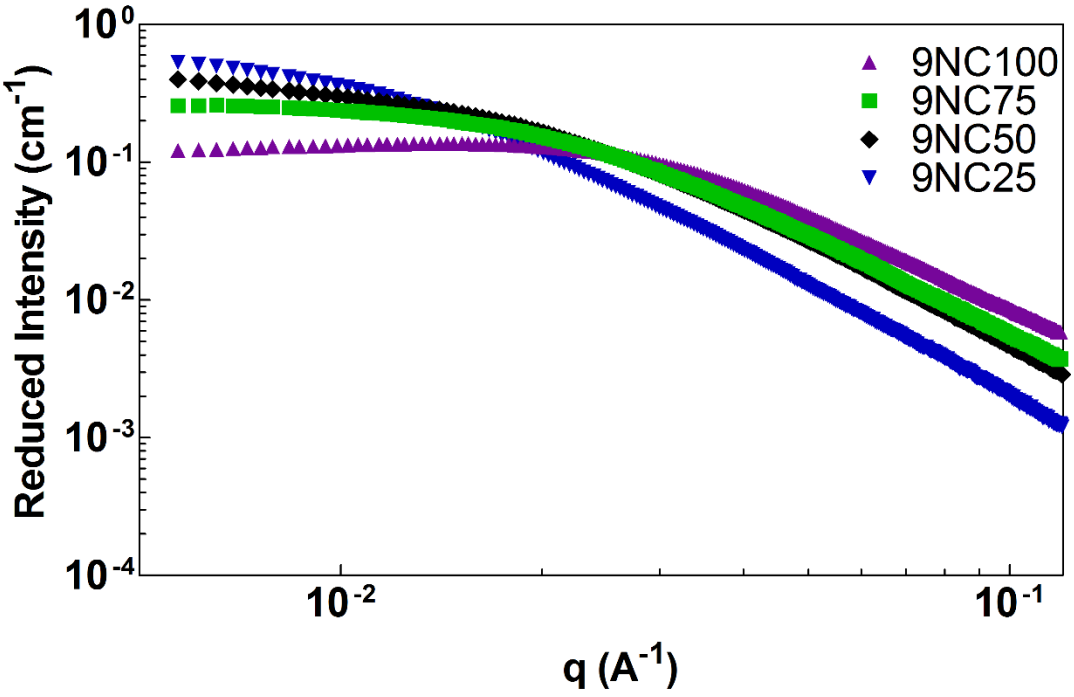

Figure S3. X-Ray Scattering indicates disk like scatterers. SAXS intensity curves of nanocomposite samples 9NC100, 9NC75, 9NC50, and 9NC25. All samples have power law decays of exponent -2 at high q, suggesting disk shaped scatterers.

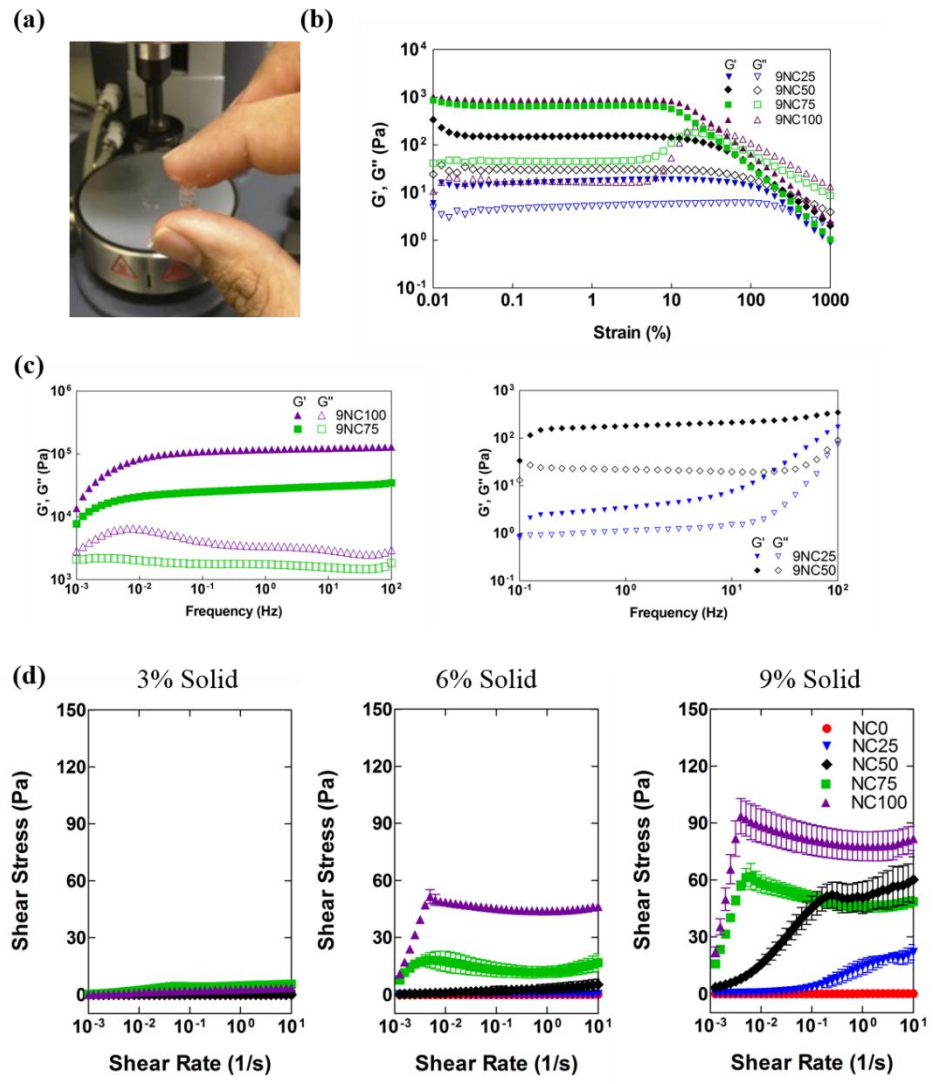

Figure S4. Linear viscoelastic range of nanocomposite hydrogels. (a) Nanocomposites are capable of being molded and are able to maintain their shape. (b) Strain sweeps indicate a crossover point (when G'=G'') that decreases with increasing silicate loading. Strain sweeps were performed at 1 Hz. (c) Frequency sweeps, at 37 °C, of 9NC25, 9NC50, 9NC75 and 9NC100 show increased moduli for higher nanoplatelet loaded nanocomposites. 9NC0 is a liquid at 37 °C and was not tested. (d) Yield stress of nanocomposites shown as a break in the linearity of shear rate *versus* shear stress plots, as a function of nanoplatelet loading and solid fraction (3%, 6% and 9 wt% solid).

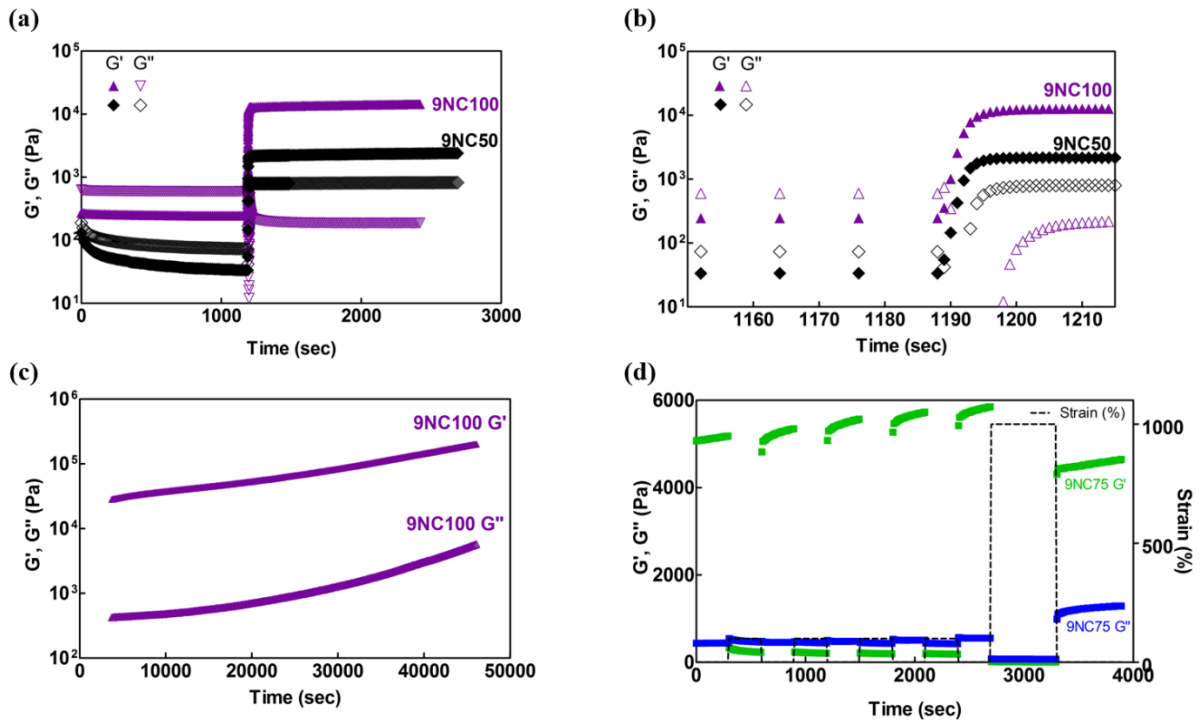

Figure S5. Nanocomposite gel recovery and aging. Recovery tests on 9NC50 and 9NC100 show rapid recovery after high oscillatory strain. Recovery was tested by straining above the crossover point, observed from strain sweeps, to break the network, resulting in G''> G', followed by removal of the strain. The a) entire test appears as an almost instantaneous recovery to solid behavior while b) an expansion of the transition region indicates the recovery takes place within a span of 10 seconds. c) Aging was observed when samples were monitored over hours at 1% strain, 1 Hz). d) This effect was able to be countered by application of high strain (1000%).

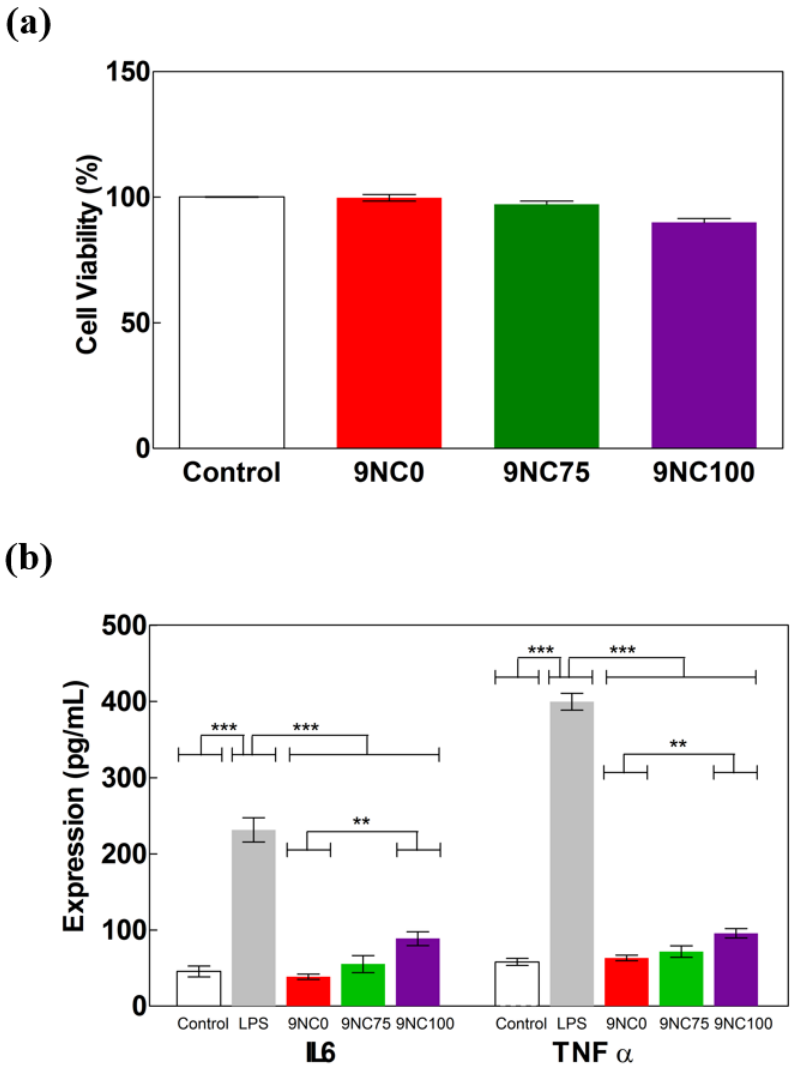

Figure S6. Injectable Gelatin/silicate hydrogel did not induce significant cytotoxic and pro-inflammatory effects in macrophages. Toxicity profiles of gelatin (9NC0), nanoplatelet gels (9NC100), and 9NC75 with RAW macrophages as determined by a) MTS assay and b) secretion of pro-inflammatory cytokines, IL-6 and TNF-α, from RAW 264.7 macrophages after 24h of exposure. (One-way Anova followed by Tukey's post hoc analysis was performed ** $p<0.01$; *** $p<0.001$)

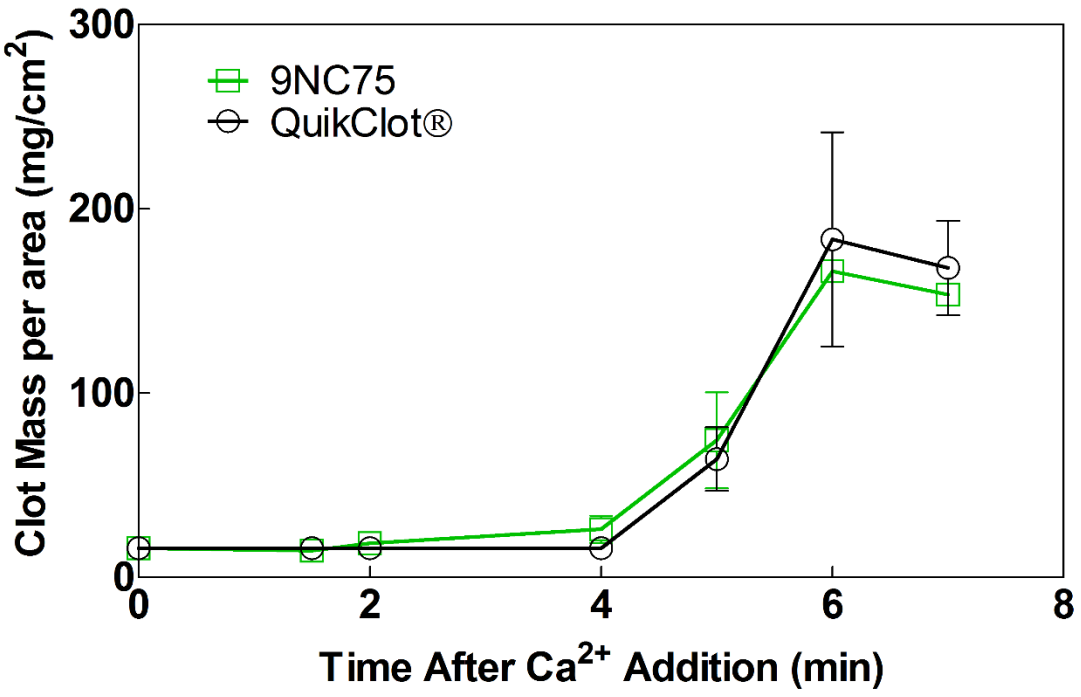

Figure S7. Time series of clot formation. Time series of thrombus weight per area for nanocomposite and hydrated QuikClot® powder show similar trends in the formation of a clot. The nanocomposite, an injectable system, begins to form a measureable clot at 2 minutes while QuikClot®, a solid hemostat, begins clotting at 5 minutes. Subsequent time points are not statistically different from one another, indicating that the ability of 9NC75 to form a clot is comparable to that of the commercial QuikClot® powder. The background mass per area of 15 mg/cm^2 is due to residual liquid remaining after the washing step is performed to halt clotting.

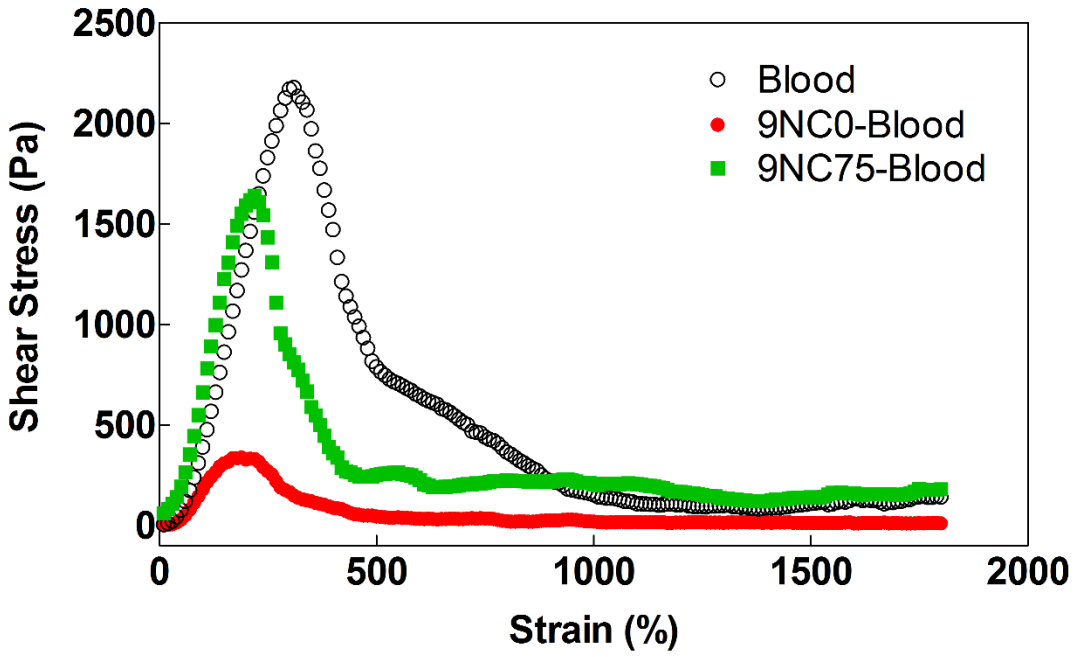

Figure S8. Effect of nanocomposite on clot strength. Rotational strain sweep of clot and clot-nanocomposite system show a decreased peak stress for clots in contact with 9NC0 in comparison to the peak stress of a clot alone. However, the peak stress for a 9NC75-clot system has a comparable peak stress to that of the clot alone.

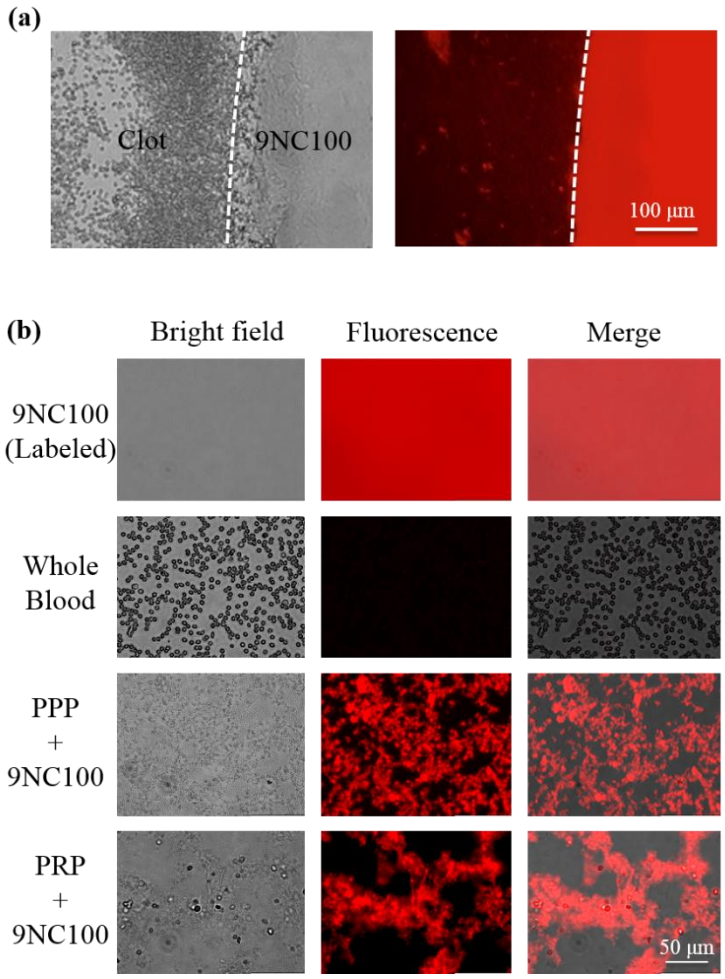

Figure S9. Nanocomposite surface initiates clotting through interactions with blood components. (a) Fluorescent imaging reveals that the interfaces between the nanocomposite and blood have localized aggregation of RBCs. (b) Silicate nanoplatelets in contact with blood proteins and RBCs were observed using fluorescently labeled silicate nanoplatelets. The presence of blood components (platelet poor plasma (PPP) or platelet rich plasma (PRP)) in the nanoplatelets disrupt their ordering, observed by the non-uniform fluorescence signal. The stability of 9NC100, previously shown by its large absolute value of zeta potential, is decreased and aggregation occurs in systems of blood components and nanocomposites, suggesting a decrease in the absolute value of the zeta potential and increase in attractive forces.

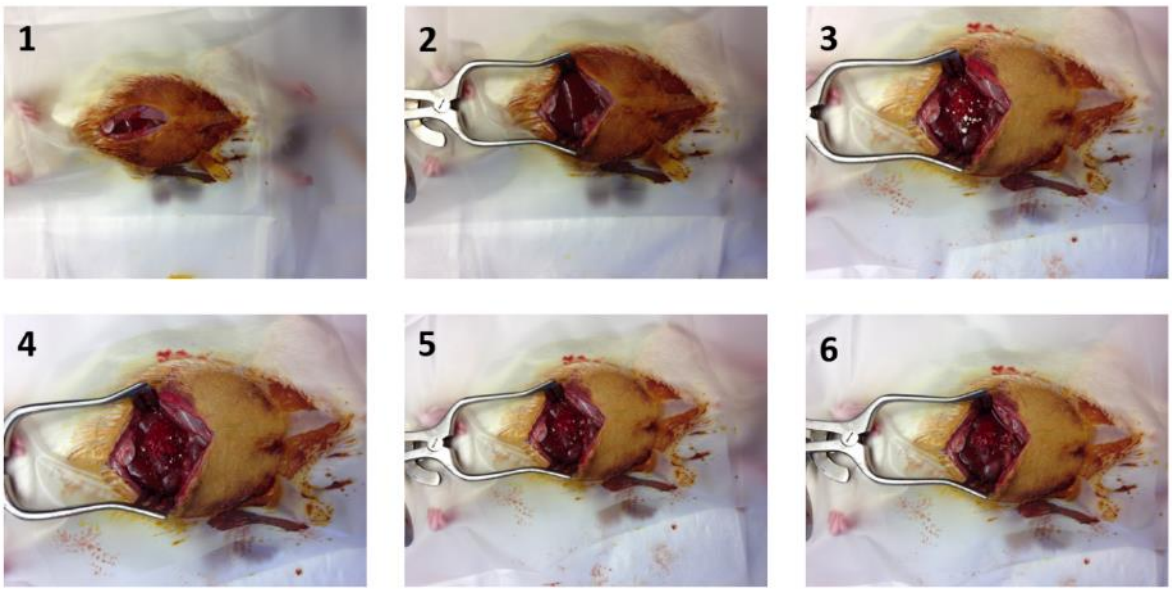

Figure S10. ***In vivo*** **procedure showing the liver bleeding model.** To induce lethal liver bleeding, the following standardized procedure was conducted prior to re-suturing: 1) median laparotomy, 2) wound edge retraction to expose the liver, 3) addition of a hemostat after laceration, 4) blood mass lost measured after two minutes, 5) blood loss measured after ten minutes and 6) saline washing of the abdominal cavity prior to resuturing. Images are from a trial with QuikClot® intervention.